



**HAL**  
open science

## Mn-Doped Ba 0.8 Sr 0.2 TiO 3 Thin Films for Energy Storage Capacitors

Caroline Borderon, Kevin Nadaud, M. Coulibaly, R. Renoud, H. Gundel

► **To cite this version:**

Caroline Borderon, Kevin Nadaud, M. Coulibaly, R. Renoud, H. Gundel. Mn-Doped Ba 0.8 Sr 0.2 TiO 3 Thin Films for Energy Storage Capacitors. International Journal of Advanced Research in Physical Science, 2019, 6 (2), pp.2349-7882. hal-02480850

**HAL Id: hal-02480850**

**<https://hal.science/hal-02480850v1>**

Submitted on 17 Feb 2020

**HAL** is a multi-disciplinary open access archive for the deposit and dissemination of scientific research documents, whether they are published or not. The documents may come from teaching and research institutions in France or abroad, or from public or private research centers.

L'archive ouverte pluridisciplinaire **HAL**, est destinée au dépôt et à la diffusion de documents scientifiques de niveau recherche, publiés ou non, émanant des établissements d'enseignement et de recherche français ou étrangers, des laboratoires publics ou privés.

## Mn-Doped Ba<sub>0.8</sub>Sr<sub>0.2</sub>TiO<sub>3</sub> Thin Films for Energy Storage Capacitors

C. Borderon<sup>1\*</sup>, K. Nadaud<sup>2</sup>, M. Coulibaly<sup>1</sup>, R. Renoud<sup>1</sup>, H.W. Gundel<sup>1</sup>

<sup>1</sup>IETR UMR CNRS 6164, Université de Nantes, 2 rue de la Houssinière, 44322 Nantes, France

<sup>2</sup>GREMAN, CNRS UMR 7347, 16 rue Pierre et Marie Curie, 37071 Tours Cedex 2, France

**\*Corresponding Author:** C. Borderon, IETR UMR CNRS 6164, Université de Nantes, 2 rue de la Houssinière, 44322 Nantes, France

### 1. INTRODUCTION

In the present paper, the influence of manganese doping on the energy storage capability of Ba<sub>0.8</sub>Sr<sub>0.2</sub>TiO<sub>3</sub> thin films is presented. The stored and recoverable energies have been calculated from the material's Polarization-electric field loop and the energy storage efficiency and figure of merit (F.O.M.) were deduced. For the undoped material, the energy loss is important and the breakdown field is low. At a suitable dopant rate, this effect disappears and a recoverable energy density of 4.4 J/cm<sup>3</sup> has been found for 1% of manganese doping. In this case, an efficiency of 93.6% and a F.O.M. of 3.82 J/cm<sup>3</sup> have been obtained. Moreover, it has been shown that the permittivity of the BST thin films doped at 1% Mn is rather stable and varies less than 2% between -80°C and 60°C, and that the dielectric losses tanδ are temperature independent and smaller than 0.014.

Today, the renewable energies replace more and more traditional fossil fuel energies implying a great demand of the associated energy storage systems. The choice of an energy storage system depends on parameters like the amount of energy to be stored and the available power, the device cost and its lifetime (number of charging - discharging cycles). In this context, ferroelectric materials seem to be good candidates because they have a high permittivity [1-3] allowing high-power energy storage applications [4]. They appear to be good competitors against super-capacitors [5], can be integrated as thin layers [5] and have a small package volume [4]. An optimal use as energy storage systems however depends on a precise control of the material's dielectric characteristics. The recoverable energy storage density per unit of volume of a ferroelectric capacitor U<sub>rec</sub> is given by [3, 4, 6]:

$$U_{rec} = \int_{P_r}^{P_{max}} E dP \quad (1)$$

where E is the applied electric field and P the polarization. P<sub>max</sub> is the maximum value of the polarization and P<sub>r</sub> is the remnant polarization. To have a high energy storage density, a large difference between P<sub>r</sub> and P<sub>max</sub> is necessary and most studies on energy-storage performances are focussed on antiferroelectric films [7-9] due to a very low remanent polarization. A high recoverable energy (32,7 J/cm<sup>3</sup>) and efficiency (~ 90%) have been obtained in Pb<sub>0.97</sub>Y<sub>0.02</sub> [(Zr<sub>0.6</sub>Sn<sub>0.4</sub>)<sub>0.925</sub>Ti<sub>0.075</sub>]<sub>0.03</sub> thin films under an applied electric field of 1800 kV/cm [7]. Relaxor ferroelectrics based on Pb(Zr,Ti)O<sub>3</sub> system are also considered and have comparable recoverable energy storage (31 J/cm<sup>3</sup>) but lower efficiency (~64%) under 2000 kV/cm [10]. These two types of antiferroelectric and relaxor ferroelectric thin films are interesting because they have a high breakdown field but all these energy storages employ lead which is poisonous to humans and environment. It is thus necessary to find lead free dielectric film with high energy storage density. Lead free Ba(1-x)<sub>x</sub>Sr<sub>x</sub>TiO<sub>3</sub> material (BST) is a soft ferroelectric for x > 0.3 which has been widely studied for its high and tunable permittivity for the realization of tunable devices [11, 12]. Recently, BST has also been considered for energy storage applications [13-15] but the energy storage density or the efficiency is still low [15, 16]. Therefore, it is desirable to improve energy storage density of BST films to have the best compromise between high energy storage density and high efficiency.

In the present study, Ba<sub>0.80</sub>Sr<sub>0.20</sub>TiO<sub>3</sub> thin films doped with manganese (Mn<sup>2+</sup>) were synthesized by Chemical Solution Deposition (CSD) and spin-coating on alumina substrates using a classical

multi-layers technique. A Ba/Sr ratio of 80/20 has been chosen because this composition has a room temperature ferroelectric phase with a Curie temperature above but close to the room temperature [17]. The typical P-E loop of this type of material is slim and the loss energy hence will be small. Manganese ions are already known to operate as electron acceptors by substituting to the titanium ions and compensate the electrons released by oxygen vacancies [18]. Mn-doping is also used to enhanced the energy storage density of lead based relaxor ferroelectric thin films [19] or paraelectric BST thin films [15]. The optimal doping rate thus depends on the material's defect density and BST doping with manganese up to 1.5% has been performed to find the best proportion by studying the P-E loops and calculating the different energies. As ferroelectric materials are also pyroelectric, the permittivity and the dielectric losses have been measured to show the stability of the dielectric properties as a function of the temperature which is fundamental for a future application. The best trade off between high released energy and low loss energy is sought.

### 2. EXPERIMENTS

Ba<sub>0.8</sub>Sr<sub>0.2</sub>TiO<sub>3</sub> thin films were realized by a sol-gel process based on the use of an alkoxide precursor. Barium acetate Ba(OOCCH<sub>3</sub>)<sub>2</sub> was mixed with strontium acetate Sr(OOCCH<sub>3</sub>)<sub>2</sub> in suitable proportions in order to obtain a Ba/Sr ratio of 80/20. Manganese acetate was added to obtain in addition BST thin films doped at 0.5, 1 and 1.5 %. The mixed powder was dissolved in acetic acid which is heated at 100°C until complete dissolution. The obtained solution was cooled down to room temperature before the addition of the titanium n-propoxide Ti(C<sub>3</sub>H<sub>7</sub>O)<sub>4</sub>. The composition was adapted in such a way to compensate for the incorporation of Mn on the Ti sites, hence resulting in a stoichiometric perovskite composition for all dopant concentrations. Ethylene glycol HO-CH<sub>2</sub>-CH<sub>2</sub>-OH was added to reduce the appearance of cracks in the film [20] and stabilize the solution [21]. Before spin-coating on platinum coated alumina substrates, the resulting solutions were filtered with a 0.2 μm PTFE filter to remove dust particles. Each solution was deposited at 4000 rpm during 20 sec and the samples were annealed during 15 min in a pre-heated open air furnace at 750°C. Multiple spin-coating was used when thicker BST layers are desired. In this work, a deposition of fourteen layers has been done.

The surface and cross-section morphology of the films were examined with a *Jeol 7600* scanning electron microscopy (SEM). X-ray diffraction (XRD) was performed for phase identification using a *Siemens D5000* diffractometer with CuK $\alpha$  radiation. Square platinum electrodes of 0.5 mm width were sputtered through a shadow mask on the films in order to form metal-ferroelectric-metal capacitors (MIM structure). The polarization versus electric field (*P-E*) hysteresis loops were measured at 1 kHz using a classical Sawyer Tower circuit. The capacitance and the dielectric loss factor ( $\tan \delta$ ) were measured using an *Agilent 4294A* at 1 kHz and 580 mV/μm and the dielectric constant of each sample was calculated.

### 3. RESULTS AND DISCUSSION

The X-ray diffraction patterns of the Ba<sub>0.8</sub>Sr<sub>0.2</sub>TiO<sub>3</sub> thin films doped from 0 to 1.5 mol% manganese are shown in Fig. 1. The peaks corresponding to the BST perovskite structure are obtained for all films which have a non-textured polycrystalline structure without preferential orientation. No parasite peak and no evidence of any secondary phase formation are visible, indicating the incorporation of the dopant into the lattice [22]. The Mn<sup>2+</sup> ion substitutes partially Ti<sup>4+</sup> on the B site as acceptor dopants in ABO<sub>3</sub> perovskite [23]. Furthermore, the diffraction angles do not shift when the dopant concentration increases, indicating that the incorporation of the Mn ion does not change the lattice parameters. This parameters are calculated on the basis of the XRD data and a value of 3.992 Å is obtained which correspond to the *a* parameter of the pseudo-cubic structure of Ba<sub>0.8</sub>Sr<sub>0.2</sub>TiO<sub>3</sub> [24]. The ionic radius of Mn<sup>2+</sup> is 670 pm, which is almost the same as the ionic radius of Ti<sup>4+</sup> (605 pm) [25].

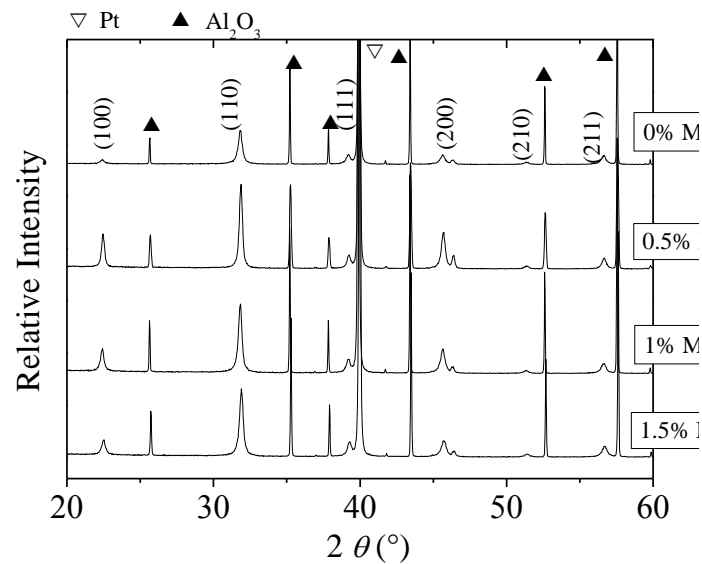


**Fig1.** X ray diffraction patterns for the  $Ba_{0.8}Sr_{0.2}TiO_3$  thin films doped with 0, 0.5, 1 and 1.5% manganese dopant.

A typical SEM cross-section of a  $Ba_{0.8}Sr_{0.2}TiO_3$  film morphology is shown in Fig. 2. All the films show a uniform, well-crystallized and void-free microstructure without cracks with an average grain size of about 60 nm. No evolution of the grain size has been found with increasing Mn content. The overall thickness of the film and of one individual layer is respectively 850 nm and 60 nm. The latter corresponds to the average grain size which effectively shows layer by layer crystallization.

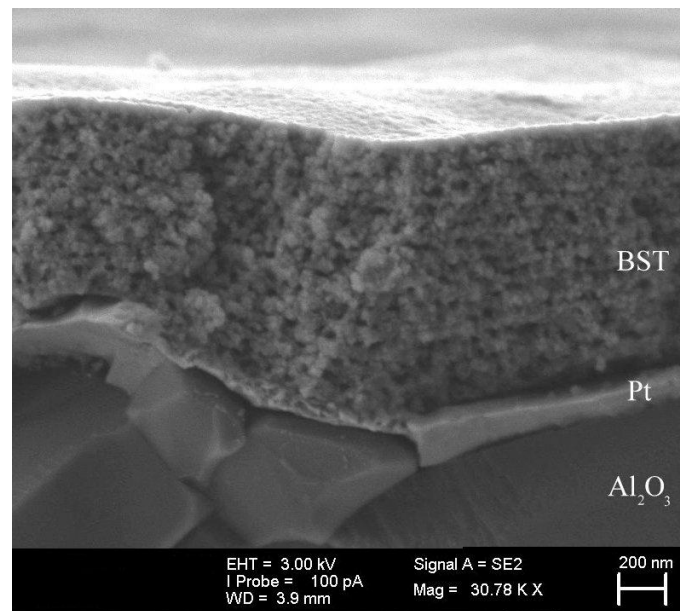


**Fig2.** SEM cross-section of the BST thin film morphology

In order to verify the effect of Mn doping on the BST ferroelectric properties, the P-E hysteresis loops of the thin films were measured at room temperature and 1 kHz (Fig. 3a-3d). All the films have been measured at their maximum value of electric field before breakdown. All the breakdown field  $E_b$  are done in the table 1. The undoped BST (Fig. 3a) does not present a pronounced ferroelectric hysteresis loop and its breakdown field is low which is probably due to a too high leakage current. The hysteresis loop of the BST doped at 0.5% (Fig. 3b) shows a slim ferroelectric loop with a very small coercive field and a remnant polarization typical of BST (80/20). The effect of doping is clearly visible as only 0.5% of manganese is sufficient to considerably reduce the losses of the material. The coercive field is 5 kV/cm and the remnant and saturation polarization are  $0.3 \mu C/cm^2$  and  $10.8 \mu C/cm^2$ , respectively, similar to what is observed for silicon substrates [26, 27]. At 1%, and 1.5% of

dopant, the breakdown field is higher (700 kV/cm for the BST doped at 1%) and the polarization at saturation is nearly 17.5  $\mu\text{C}/\text{cm}^2$  for the two samples, showing that defects like oxygen vacancies are neutralized by doping. The coercive field is slightly higher for the two samples ( $E_c \approx 9 \text{ kV}/\text{cm}$ ) and at 1.5% Mn, the hysteresis loop is more opened showing that additional defects were created in the material.

**Table1.** Ferroelectric and energy storage properties of doped and undoped BST thin films.

| Samples  | $E_b$ (kV/cm) | $P_{max}$ ( $\mu\text{C}/\text{cm}^2$ ) | $U_{rec}$ ( $\text{J}/\text{cm}^3$ ) | $\square$ (%) |
|----------|---------------|---|--------------------------------------|---------------|
| BST 0%   | 150           | 6.9                                     | 0.45                                 | 45.9          |
| BST 0.5% | 520           | 10.6                                    | 2.13                                 | 94.4          |
| BST 1%   | 730           | 17.5                                    | 4.36                                 | 93.6          |
| BST 1.5% | 600           | 17.6                                    | 4.24                                 | 92.2          |

The P-E loops allow us to calculate the recoverable energy  $U_{rec}$  and the stored energy  $U_s$  and these energies are shown in Fig. 4 for all doping rates. The stored energy is the integration between the charge curve and polarization axis and the recoverable energy between the discharge curve and polarization axis. For the undoped sample,  $U_s$  and  $U_{rec}$  are small due to the important conduction losses in the material and the low breakdown field. When introducing the Mn<sup>2+</sup> ions, the loop becomes thinner and the energy loss is considerably reduced, as a consequence the stored and released energies become similar. However, the sample doped at 0.5% presents a lower breakdown field than the BST doped at 1% and the maximum energy released remains low ( $U_{rec} = 2,13 \text{ J}/\text{cm}^3$ ). As a consequence, the released energy initially raises, attains a maximum near 1% doping rate and then slightly decreases, following the evolution of the breakdown field. The highest released energy is found for 1% of manganese and is equal to  $4.36 \text{ J}/\text{cm}^3$ . This value is in agreement with the measured and calculated energy density of Ba<sub>0.8</sub>Sr<sub>0.2</sub>TiO<sub>3</sub> ceramic material for a maximum electric field of 700 kV/cm [3].

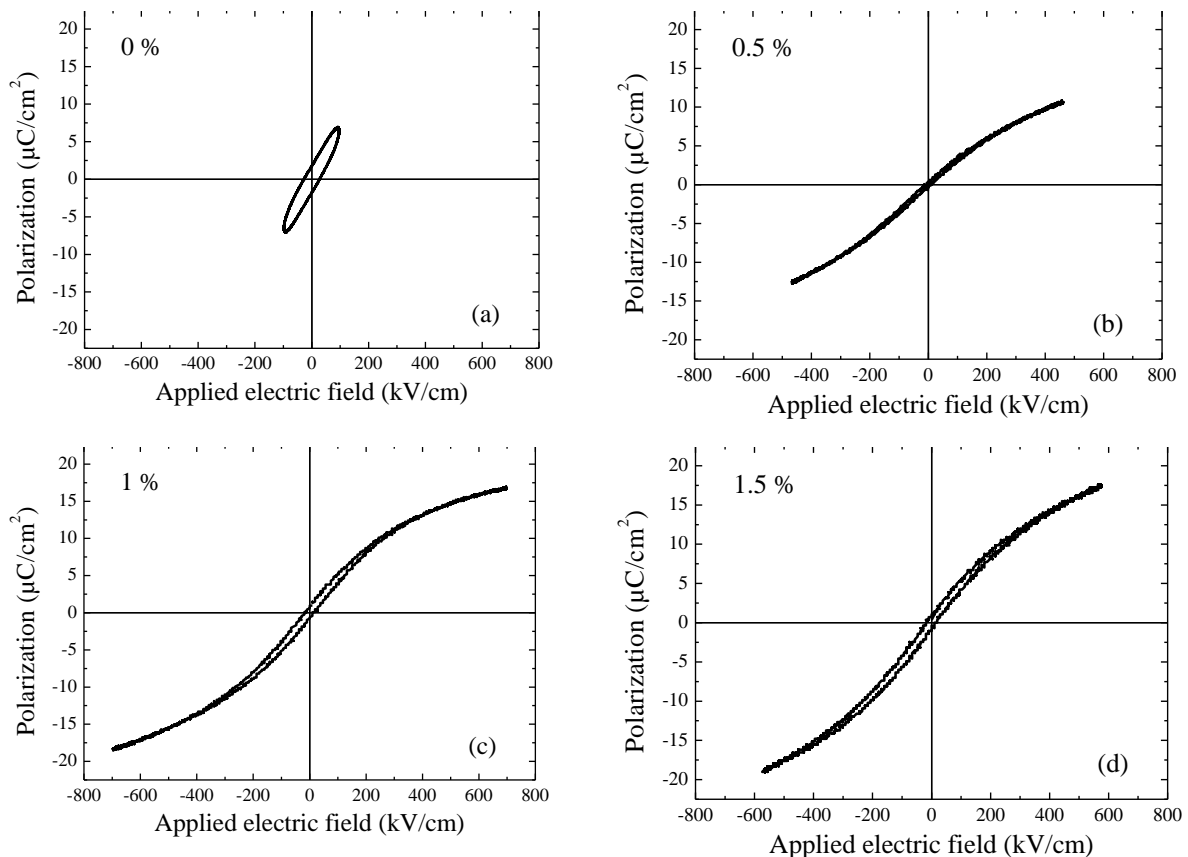


**Fig3.** Hysteresis loop P-E of the BST thin films doped at (a) 0%, (b) 0.5%, (c) 1 %, and (d) 1.5% of manganese

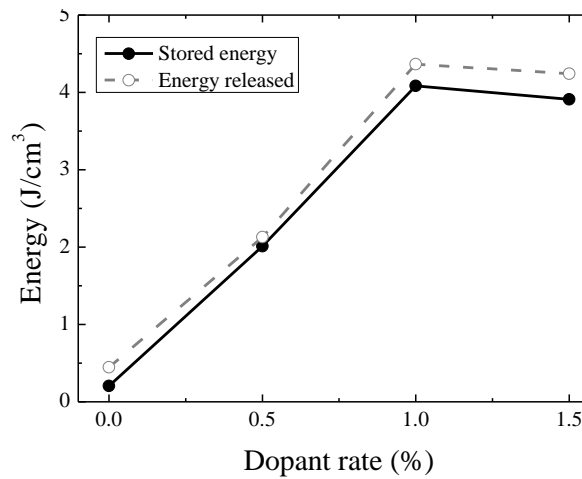


**Fig4.** Stored energy and energy released as a function of the doping rate

To qualify the energy storage efficiency, the proportion of the charge energy which is released is determined by [4, 15]:

$$\eta(\%) = \frac{U_{rec}}{U_s} \times 100 \tag{2}$$

The efficiency as a function of the dopant rate is shown in the Fig. 5. As the hysteresis loops is slimmer when the dopant rate reaches 0.5%, the efficiency is maximum. An efficiency of 94.4%, 93.6% and 92.2% has been found for the BST doped at 0.5%, 1% and 1.5%, respectively. These values are higher than the efficiency reported on other materials such as {Ba(Zr<sub>0.2</sub>Ti<sub>0.8</sub>)O<sub>3</sub>}(1-x){(Ba<sub>0.7</sub>Ca<sub>0.3</sub>)TiO<sub>3</sub>}<sub>x</sub> ceramics (72 % maximum) [28], BaTiO<sub>3</sub>/Ba<sub>1-x</sub>Sr<sub>x</sub>TiO<sub>3</sub> relaxor-ferroelectric superlattices (59 to 67%) [29] or Ba<sub>0.4</sub>Sr<sub>0.6</sub>TiO<sub>3</sub> thin films (35.6 to 48.5%)[15]. However a high efficiency is not profitable if the released energy is weak as for the BST doped at 0.5%. Hence a figure of merit (F.O.M.), taking into account the trade off between a high released energy and a low consuming energy, can be defined:

$$F.O.M. = \eta \times U_{rec} \tag{3}$$

The higher the F.O.M. is, the more efficient is the energy storage device. In our case, the highest F.O.M. is found for the BST doped at 1%. For a lower dopant rate, even if the efficiency is high, the energy release is not enough important. For a dopant rate higher than 1%, the losses are low but the released energy is lower too due to additional defects created in the material. The BST doped at 1% presents an efficiency of 93.6% and a F.O.M. of 3.82 J/cm<sup>3</sup> which is higher to what is reported in [28] (0.68 J/cm<sup>3</sup>) but lower to [29] (7.0 J/cm<sup>3</sup>) due to a smaller released energy and a smaller applied electric field.

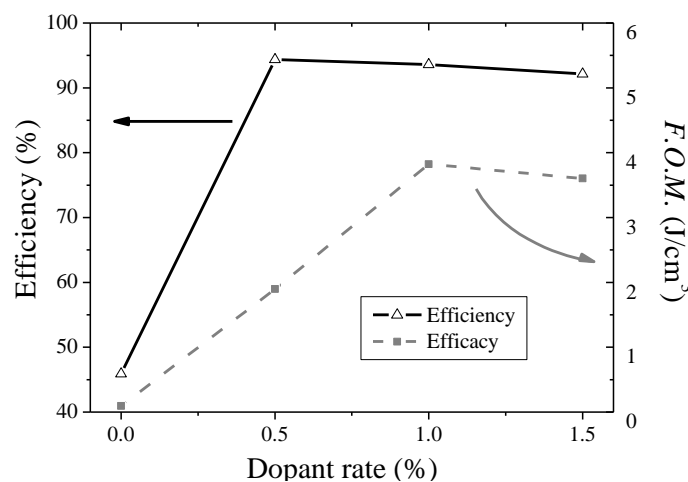


**Fig5.** Efficiency and F.O.M. of the BST thin films as a function of the dopant rate.

For a future energy storage application, the ferroelectric thin films must be stable in a large temperature range around the ambient temperature. The relative permittivity and the dielectric losses as a function of temperature are shown in Fig. 6 to know the stability of the BST thin films. The value of the permittivity decreases with the dopant rate which is attributed to the increasing number of nonferroelectric cells when incorporating the dopant into the material [12]. All films present the same evolution and show the non sensibility to doping. Contrary to a single-crystal, there is no abrupt ferroelectric - paraelectric phase transition and the evolution of the relative permittivity is smooth, which has already been reported in [12, 30]. This slow temperature evolution is due to the absence of a preferential orientation (Fig.1), the quite small grain size (Fig. 2), and the substrate which induces stress in the film [26]. In the ferroelectric phase, below 60°C, the relative permittivity is quite stable, but at higher temperatures, in the paraelectric phase, it significantly drops with a slope of  $-0.9^{\circ}\text{C}^{-1}$ . The dielectric losses do not show a significant evolution as a function of the temperature but depend on the dopant rate as already visible from the hysteresis loops (Fig .3). The dielectric losses decrease for doping up to 1% and increase again when the amount of the dopant becomes more important since new defects are created. The minimum dielectric losses at 1% addition of manganese were smaller than 0.014, again confirming this optimum doping rate.

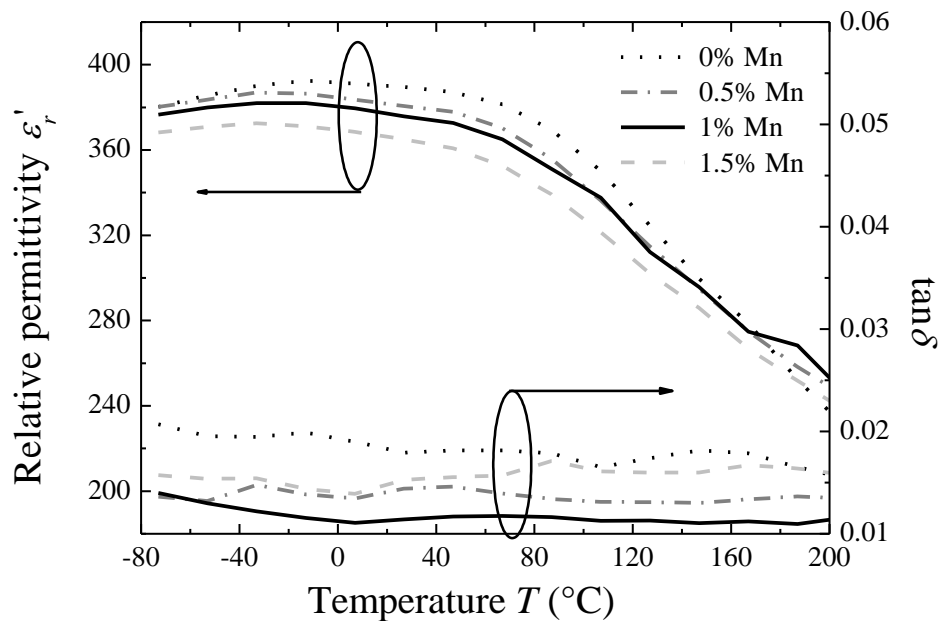


**Fig6.** Relative permittivity and dielectric losses of doped and undoped BST thin films at 1 kHz and as a function of the temperature.

As the permittivity of ferroelectrics is generally temperature dependent and varies especially near to the Curie temperature, it is important to indicate the temperature stability of the elaborated thin films which is quantified by the Temperature Coefficient Capacitance (TCC) [13]:

$$TCC(\%) = \frac{|\varepsilon_r'(T) - \varepsilon_r'(25^{\circ}\text{C})|}{\varepsilon_r'(25^{\circ}\text{C})} \times 100 \quad (4)$$

with  $\varepsilon_r'(T)$  the relative permittivity at the temperature T and  $\varepsilon_r'(25^{\circ}\text{C})$  the reference value of the relative permittivity at room temperature (25°C). The TCC(%) is represented as a function of the temperature for all dopants in Fig. 7, also indicating the 2% variation limit of high value commercial capacitors [31]. For all dopants, the variation of the material's relative permittivity is less than 2% from -80°C to +60°C. The corresponding temperature interval of 140°C is larger than what it is reported in literature [32, 33] and shows the good stability of the BST thin film dielectric properties as the function of temperature which fundamental for energy storage application.

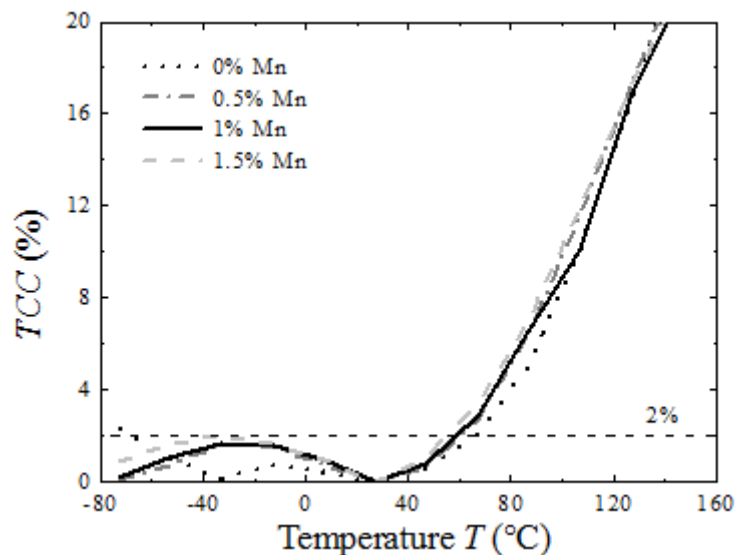


**Fig8.** Temperature coefficient capacitance of the doped and undoped BST thin films as a function of temperature

#### 4. CONCLUSION

Substitution at the B-site of the perovskite lattice of Ba<sub>0.80</sub>Sr<sub>0.20</sub>TiO<sub>3</sub> (BST 80/20) thin films by Mn<sup>2+</sup> ions has been investigated to study the effect of the doping on the energy storage properties. The BST 80/20 composition is located near to the ferroelectric-paraelectric structural phase boundary and hence has a slim ferroelectric loop. Introduction of a small amount of the manganese dopant prevents diffusion due to oxygen vacancies since manganese is an electron acceptor and hence considerable reduction of the losses is observed. The breakdown field is then higher for 1% of Mn doping and a recoverable storage energy of 4.4 J/cm<sup>3</sup> is found. Doping with 1% manganese results also in an optimum figure of merit as the efficiency is 93.6%.

Moreover, it has been shown that the dielectric properties of the BST thin films are rather stable over a large temperature range. The permittivity varies less than 2% between -80°C and 60°C and the dielectric losses are rather temperature independent and smaller than 0.014 in the totally temperature range for the BST doped at 1%.

#### REFERENCES

- [1] Y. Jianding, P.F. Paradis, T. Ishikawa, S. Yoda, Y. Saita, M. Itoh, F. Kano, Giant dielectric constant of hexagonal BaTiO<sub>3</sub> crystal grown by containerless processing, *Chemistry of Materials*, 16 (2004) 3973-3975.
- [2] K. Zelonka, M. Sayer, A.P. Freundorfer, J. Hadermann, Hydrothermal processing of barium strontium titanate sol-gel composite thin films, *Journal of Materials Science*, 41 (2006) 3885-3897.
- [3] H.N. Fletcher, A.D. Hilton, B.W. Ricketts, Optimization of energy storage density in ceramic capacitors, *Journal of Physics D: Applied Physics*, 29 (1996) 253-258.
- [4] S. Tong, B. Ma, M. Narayanan, S. Liu, R. Koritala, U. Balachandran, D. Shi, Lead Lanthanum Zirconate Titanate Ceramic Thin Films for Energy Storage, *ACS Applied Materials & Interfaces*, 5 (2013) 1474-1480.
- [5] K. Yao, S. Chen, M. Rahimabady, M. Mirshekarloo, S. Yu, F. Tay, T. Sritharan, L. Lu, Nonlinear dielectric thin films for high-power electric storage with energy density comparable with electrochemical supercapacitors, *IEEE Trans Ultrason Ferroelectr Freq Control.*, 58 (2011) 1968-1974.
- [6] X. Hao, A review on the dielectric materials for high energy-storage application, *Journal of Advanced Dielectrics*, 03 (2013) 1330001.
- [7] C.W. Ahn, G. Amarsanaa, S.S. Won, S.A. Chae, D.S. Lee, I.W. Kim, Antiferroelectric Thin-Film Capacitors with High Energy-Storage Densities, Low Energy Losses, and Fast Discharge Times, *ACS Applied Materials & Interfaces*, 7 (2015) 26381-26386.
- [8] I.V. Ciuchi, L. Mitoseriu, C. Galassi, Antiferroelectric to Ferroelectric Crossover and Energy Storage Properties of (Pb<sub>1-x</sub>La<sub>x</sub>)(Zr<sub>0.90</sub>Ti<sub>0.10</sub>)<sub>1-x/4</sub>O<sub>3</sub> (0.02 ≤ x ≤ 0.04) Ceramics, *Journal of the American Ceramic Society*, 99 (2016) 2382-2387.



- [9] M.S. Mirshekarloo, K. Yao, T. Sritharan, Large strain and high energy storage density in orthorhombic perovskite (Pb<sub>0.97</sub>La<sub>0.02</sub>)(Zr<sub>1-x</sub>Sn<sub>x</sub>Ti<sub>y</sub>)O<sub>3</sub> antiferroelectric thin films, *Applied Physics Letters*, 97 (2010) 142902.
- [10] X. Wang, L. Zhang, X. Hao, S. An, B. Song, Dielectric properties and energy-storage performances of (1-x)Pb(Mg<sub>1/3</sub>Nb<sub>2/3</sub>)O<sub>3</sub> relaxor ferroelectric thin films, *Journal of Materials Science: Materials in Electronics*, 26 (2015) 9583-9590.
- [11] H.V. Nguyen, R. Benzerga, C. Borderon, C. Delaveaud, A. Sharaiha, R. Renoud, C. Le Paven, S. Pavy, K. Nadaud, H.W. Gundel, Miniaturized and reconfigurable notch antenna based on a BST ferroelectric thin film, *Materials Research Bulletin*, 67 (2015) 255-260.
- [12] K. Nadaud, C. Borderon, R. Gillard, E. Fourn, R. Renoud, H.W. Gundel, Temperature stable BaSrTiO<sub>3</sub> thin films suitable for microwave applications, *Thin Solid Films*, 591, Part A (2015) 90-96.
- [13] S. Chao, F. Dogan, BaTiO<sub>3</sub>=SrTiO<sub>3</sub> layered dielectrics for energy storage, *Materials Letters*, 65 (2011) 978-981.
- [14] G. Dong, S. Ma, J. Du, J. Cui, Dielectric properties and energy storage density in ZnO-doped Ba<sub>0.3</sub>Sr<sub>0.7</sub>TiO<sub>3</sub> ceramics, *Ceramics International*, 35 (2009) 2069-2075.
- [15] C. Diao, H. Liu, H. Hao, M. Cao, Z. Yao, Enhanced recoverable energy storage density of Mn-doped Ba<sub>0.4</sub>Sr<sub>0.6</sub>TiO<sub>3</sub> thin films prepared by spin-coating technique, *Journal of Materials Science: Materials in Electronics*, 29 (2018) 5814-5819.
- [16] Q. Luo, X. Li, Z. Yao, L. Zhang, J. Xie, H. Hao, M. Cao, A. Manan, H. Liu, The role of dielectric permittivity in the energy storage performances of ultrahigh-permittivity (Sr<sub>x</sub>Ba<sub>1-x</sub>)(Ti<sub>0.85</sub>Sn<sub>0.15</sub>)O<sub>3</sub> ceramics, *Ceramics International*, 44 (2018) 5304-5310.
- [17] V.V. Lemanov, E.P. Smirnova, P.P. Syrnikov, E.A. Tarakanov, Phase transitions and glasslike behavior in Sr<sub>1-x</sub>Ba<sub>x</sub>TiO<sub>3</sub>, *Physical Review B (Condensed Matter)*, 54 (1996) 3151-3157.
- [18] K. Nadaud, C. Borderon, R. Renoud, H.W. Gundel, Effect of manganese doping of BaSrTiO<sub>3</sub> on diffusion and domain wall pinning, *Journal of Applied Physics*, 117 (2015) 084104.
- [19] Y. Liu, X. Hao, S. An, Significant enhancement of energy-storage performance of (Pb<sub>0.91</sub>La<sub>0.09</sub>)(Zr<sub>0.65</sub>Ti<sub>0.35</sub>)O<sub>3</sub> relaxor ferroelectric thin films by Mn doping, *Journal of Applied Physics*, 114 (2013) 174102.
- [20] N.V. Giridharan, S. Madeswaran, R. Jayavel, Structural, morphology and electrical studies on ferroelectric bismuth titanate thin films prepared by sol-gel technique, *J. Cryst. Growth*, 237-239 (2002) 468-472.
- [21] H.-Y. Tian, W.-G. Luo, X.-H. Pu, X.-Y. He, P.-S. Qiu, A.-L. Ding, Synthesis and dielectric characteristic of Ba<sub>1-x</sub>Sr<sub>x</sub>TiO<sub>3</sub> thin films-based strontium-barium alkoxides derivatives, *Materials Chemistry and Physics*, 69 (2001) 166-171.
- [22] W. Hofman, S. Hoffmann, R. Waser, Dopant influence on dielectric losses, leakage behaviour, and resistance degradation of SrTiO<sub>3</sub> thin films, *Thin Solid Films*, 305 (1997) 66-73.
- [23] W.J. Jie, J. Zhu, W.F. Qin, X.H. Wei, J. Xiong, Y. Zhang, A. Bhalla, Y.R. Li, Enhanced dielectric characteristics of preferential (1 1 1)-oriented BZT thin films by manganese doping, *Journal of Physics D (Applied Physics)*, 40 (2007) 2854-2857.
- [24] B.A. Baumert, L.-H. Chang, A.T. Matsuda, T.-L. Tsai, C.J. Tracy, R.B. Gregory, P.L. Fejes, N.G. Cave, W. Chen, D.J. Taylor, T. Otsuki, E. Fujii, S. Hayashi, K. Suu, Characterization of sputtered barium strontium titanate and strontium titanate-thin films, *Journal of Applied Physics*, 82 (1997) 2558-2566.
- [25] R.D. Shannon, C.T. Prewitt, Effective ionic radii in oxides and fluorides, *Acta Crystallographica, Section B (Structural Crystallography and Crystal Chemistry)*, B25 (1969) 925-946.
- [26] J.-G. Cheng, X.-J. Meng, B. Li, J. Tang, S.-L. Guo, J.-H. Chu, M. Wang, H. Wang, Z. Wang, Ferroelectricity in sol-gel derived Ba<sub>0.8</sub>Sr<sub>0.2</sub>TiO<sub>3</sub> thin films using a highly diluted precursor solution, *Applied Physics Letters*, 75 (1999) 2132-2134.
- [27] T.J. Zhang, H. Ni, W. Wang, Preparation and characterization of epitaxial-grown Ba<sub>0.65</sub>Sr<sub>0.35</sub>TiO<sub>3</sub> thin films by the sol-gel process on Pt/MgO substrates, *Journal of Materials Synthesis and Processing*, 10 (2002) 17-21.
- [28] V.S. Puli, D.K. Pradhan, D.B. Chrisey, M. Tomozawa, G.L. Sharma, J.F. Scott, R.S. Katiyar, Structure, dielectric, ferroelectric, and energy density properties of (1-x)BZT-xBCT ceramic capacitors for energy storage applications, *Journal of Materials Science*, 48 (2013) 2151-2157.
- [29] N. Ortega, A. Kumar, J.F. Scott, B.C. Douglas, M. Tomazawa, K. Shalini, D.G.B. Diestra, R.S. Katiyar, Relaxor-ferroelectric superlattices: high energy density capacitors, *Journal of Physics: Condensed Matter*, 24 (2012) 445901.

- [30] T.M. Shaw, Z. Suo, M. Huang, E. Liniger, R.B. Laibowitz, J.D. Baniecki, The effect of stress on the dielectric properties of barium strontium titanate thin films, *Applied Physics Letters*, 75 (1999) 2129-2131.
- [31] A.T. Ceramics, 116 series Microcaps®, 2015.
- [32] M.P.J. Tiggelman, K. Reimann, M. Klee, R. Mauczock, W. Keur, R.J.E. Hueting, Ba<sub>x</sub>Sr<sub>1-x</sub>Ti<sub>1.02</sub>O<sub>3</sub> metal-insulator-metal capacitors on planarized alumina substrates, *Thin Solid Films*, 518 2854-2859.
- [33] M. Jain, S.B. Majumder, R.S. Katiyar, F.A. Miranda, F.W. Van Keuls, Improvement in electrical characteristics of graded manganese doped barium strontium titanate thin films, *Applied Physics Letters*, 82 (2003) 1911-1913.

**Citation:** C. Borderon. "Mn-Doped Ba<sub>0.8</sub>Sr<sub>0.2</sub>TiO<sub>3</sub> Thin Films for Energy Storage Capacitors", *International Journal of Advanced Research in Physical Science (IJARPS)*, vol. 6, no. 2, pp. 1-9, 2019.

**Copyright:** © 2019 Authors, This is an open-access article distributed under the terms of the Creative Commons Attribution License, which permits unrestricted use, distribution, and reproduction in any medium, provided the original author and source are credited.